THE ROLE OF THE TERRAIN GEOMETRY ON THE FLAMES PROPAGATION THROUGH A VEGETATIVE FUEL BED

L. Malangone P. Russo and S. Vaccaro
lmalangone@unisa.it
Department of Industrial Engineering, University of Salerno, Fisciano (SA), Italy

Abstract
When a wildland fire occurs the domain geometry is a key parameter in governing the way the fire spreads across the terrain. The effect of this variable on the rate of flames propagation was investigated in this work by means of a computational fluid dynamics software specifically designed to simulate fires in wildland environment. The physics-based model - i.e. relied on the laws of conservation of momentum, energy and mass – was adopted under two different domain configurations (double-slope domains and canyon); the capability of the computational code to correctly predict the fire behaviour was verified by comparison with results of experimental tests available in the literature.

1. Introduction
Mathematical simulation of wildland fires is a very complex task. The rate of spread and the shape of forest fire fronts have been studied by many researchers [1, 2, ,3, 4; 5] who noticed that they are affected by many factors such as fuel type and its moisture content, wind velocity, forest topography, fuel distribution. The formulated models used for fire modelling are usually classified into empirical models, which are based primary on statistics collected by observations of experimental or historical fires; physical models based on physical principles of fluid dynamic and laws of conservation of energy and mass; semi empirical models, based on physical laws, but enhanced with some empirical factors.

Although the last approach may appear reasonable to consider being a good compromise between the first two, it is not always able to give good predictions of the behaviour of wildfires in particular situations, such as for heterogeneous vegetations, for crown fires or when slope and wind effects are combined [6]. Therefore, considering also the always-growing improvements offered by computer potentiality, fully physical approach received great interest in this last decade [7, 8, 9, 10, 11] and models able to consider strong interactions between phenomena in the gaseous phase - such as the turbulence in the lower part of the atmospheric boundary layer, chemical reactions and radiation heat transfer in the flaming zone - started to be considered. However, even if this new approach is based on the resolution of well known balance equations (mass, momentum, energy) governing the evolution of the state of the vegetation and of the surrounding atmosphere, due to the coupling of non-linear phenomena, the development of such models remains very complex and the numerical results need to be validated by comparisons with experimental data. Moreover, in contrast with empirical models, which application is limited to systems and to operating conditions for which the model is generated, complete physical models do not have this limitation: they can be adopted in different geometries and for different boundary conditions, but requires input data to be accurate.

The effect of geometry on flame propagation was investigated by many authors who focused their attention especially on flame moving on flat or sloped surfaces under calm and windy conditions [11, 12, 13, 14, 15, 16]: in these cases the fire spreading rate results substantially constant when the main parameters governing the phenomenon (domain inclination, vegetation and meteorology) remain unchanged. However, recent works [17, 18]

showed that such a condition is not true when particular geometric configurations are considered (i.e. valley, canyon): even in absence of wind, the fire rate of spread may become not constant in the time nor uniform in the space making the actual fire propagation rate more complex to identify and less predictable. This work aimed at investigating the ability of a physics-based model to adequately simulate experimental results and to correctly reproduce the way fire spreads across two different terrain configurations (double-slope domains and canyon) in the absence of wind; this was accomplished by comparing the results of the model simulations with findings from experimental tests available in the literature [17, 18]. In the simulations, the vegetative fuel is arranged in beds of different inclinations and fire propagates across them according to terrain inclination and shape The combined contribution of these two parameters determines the position of the flame with respect to the fuel: an abrupt change in slope makes the rate of flame propagation dependent also on the fire evolution history, while a canyon configuration induces a transient rate of spread whose duration cannot be defined *a priori*.

2. Mathematical model

WFDS is the mathematical code used to perform fire simulations. It is a physics-based code developed by NIST (National Institute of Standard and Technology) as an extension of an already existing software for the simulation of fire propagation in enclosures (FDS). WFDS is a modified version of FDS able to perform simulations in forest-like environment, but build on the same mathematical architecture of FDS. The main references for this code are from Hinze [19], who described the equations and in-depth theory behind turbulence, McGrattan et al. [20], who provided the actual equations used in FDS and Cox [21], who presented the derivations and basic concepts for the conservation equations and turbulence modelling. A comprehensive discussion of the FDS code will not be provided in this paper, but only a brief overview of the model will be presented.

FDS solves the Navier-Stokes equations in the case of low Mach numbers [22]. This simplified form is achieved by filtering out acoustic waves allowing for large variations in density and temperature but only small changes in pressure, which are typical of fire scenarios. As described in McGrattan et al. [20], the governing equations, before to apply the simplifications consistent with the low Mach number assumption, are the balances for mass, species, momentum and energy.

Mass: $$\frac{\partial \rho}{\partial t} + \nabla \cdot \rho \vec{u} = \dot{m}_b''' \tag{1}$$

Species: $$\frac{\partial}{\partial t}\left(\rho Y_\alpha\right) + \nabla \cdot \rho Y_\alpha \vec{u} = \nabla \cdot \rho D_\alpha \nabla Y_\alpha + \dot{m}_\alpha''' + \dot{m}_{b,\alpha}''' \tag{2}$$

Momentum: $$\rho\left(\frac{\partial \vec{u}}{\partial t} + \left(\vec{u} \cdot \nabla\right)\vec{u}\right) + \nabla p = \rho \vec{g} + \vec{f} + \nabla \cdot \hat{\tau} \tag{3}$$

Energy: $$\frac{\partial}{\partial t}\left(\rho h_s\right) + \nabla \cdot \rho h_s \vec{u} - \frac{\partial p}{\partial t} - \vec{u} \cdot \nabla p = \\ = \dot{q}''' - \dot{q}_b''' - \nabla \cdot \dot{q}_r'' + \nabla \cdot k \nabla T + \nabla \cdot \sum_\alpha h_{s,\alpha} \rho D_\alpha \nabla Y_\alpha + \varepsilon \tag{4}$$

In the equations (1) and (2) $\dot{m}_b''' = \sum_\alpha \dot{m}_{b,\alpha}'''$ is the production rate of species by evaporating droplets or particles. Summing the equation (2) over all species, yields the original mass conservation equation, being $\sum Y_\alpha = 1$, $\sum \dot{m}_\alpha''' = 0$ and $\sum \dot{m}_{b,\alpha}''' = \dot{m}_b'''$ by

definition, and because it is assumed that $\sum \rho D_\alpha \nabla Y_\alpha = 0$. These transport equations are solved for total mass and all but one of the species, implying that the diffusion coefficient of the implicit species is chosen so that the sum of all the diffusive fluxes is zero. In the equation (3) the forces in the second half of the expression include gravity ($\vec{g}$), an external drag force vector ($\vec{f}$) [10] and a measure of the viscous stress ($\hat{\tau}$) acting on the fluid within the control volume. Of these three forces, gravity is the most important because it represents the influence of buoyancy on the flow. In the equation (4), $\dot{q}'''$ is the heat release rate per unit volume from a chemical reaction, $\dot{q}_b'''$ is the energy transferred to the evaporating droplets, $\dot{q}_r'''$ is the radiative heat flux, ε is the dissipation rate, k is the thermal conductivity and D_α is the diffusion coefficient.

The equation of state used for problem closure is the ideal gas law with a term added to account for the atmospheric density gradient and a flow induced perturbation pressure term. The mode of simulation in FDS depends on the grid resolution: Large Eddy Simulation (LES) and Direct Numerical Simulation (DNS). For the LES approach to fire modelling, where the grid resolution is not fine enough to capture all the relevant mixing processes, the sub-grid analysis of Smagorinsky is used to model the viscosity [20].

For modelling the burning of solid phases, several parameters must be included in the code, such as surface/volume ratio, moisture content, char fraction and bulk density. WFDS assumes a two-stage endothermic thermal decomposition (water evaporation and, then, solid fuel pyrolysis). It uses the temperature dependent mass loss rate expression of Morvan and Dupuy [11] to model the solid fuel degradation and assumes that pyrolysis occurs at 127°C. Solid fuel is represented as a series of layers that are consumed from the top down until the solid mass reaches a predetermined char fraction at which point the fuel is considered consumed.

For gas-phase combustion LES calculation refers to the turbulent mixing of combustion gases with the surrounding atmosphere assuming that the mixing controls combustion and all species of interest can be represented by a single variable known as the mixture fraction (*Z*). *Z* is derived from a linear combination of fuel and oxygen mass transport equations and represents the fraction of fuel/oxygen in a given point. In any case, it is a quantity that satisfies the conservation equation. The mass fractions of all of the major reactants and products can be deduced from the mixture fraction by means of expressions obtained by a combination of simplified analysis and measurement.

3. Mesh sensitivity

The different phenomena involved in forest fire modelling cover an extremely variety of length and time scales, making almost impossible the definition of a single set of scaling parameters. The most classic attempts for scaling are associated with pool fires, entrainment and compartment fires, reviewed to a great extent by Zukoski [23]. The main parameter from Zukoski's analysis is

$$Q^* = \frac{\dot{Q}}{\rho_\infty C_P T_\infty (gD)^{1/2} D^2} \tag{5}$$

Where $\dot{Q}$ is the energy release rate issued from the combustion process and ρ_∞, C_p and T_∞ are the ambient air density, specific heat and temperature, respectively. g is the gravity vector and *D* is the diameter or characteristic length scale of the fire. *Q** represents the ratio between the energy provided by the combustion reaction and the energy associated with the

induced buoyant flow. The relation between D and the buoyantly induced velocity (u_b) is defined as $u_b = \sqrt{gD}$ with the assumption that the pool diameter is the characteristic length scale of the problem. A different approach consists in considering Q^* equal to one and extract the characteristic length scale (D) from Equation (5):

$$D = \left(\frac{\dot{Q}}{\rho_\infty C_P T_\infty \sqrt{g}} \right)^{2/5} \tag{6}$$

The length scale D can then be successfully used to scale the characteristic flame diameter at the axis of a pool fire, but it implies that motion is purely dominated by buoyancy. Therefore, it is limited when either fuel injection velocity (jets), geometry (confinement) or length scale (flow instabilities) introduce other driving forces to the problem. For the simulations considered in this work the mesh resolution was set by the dimensionless ratio D/δ_x [24]. The quantity D/δ_x can be considered as the number of computational cells spanning the characteristic diameter of the fire; values for D/δ_x, useful to get a good resolution of the calculation, ranges from 4 to 16. A value of about 16 of such a ratio was chosen for the canyon simulations implying a maximum mesh size of 0.03 m. In the double-slope domains simulations, instead, the D/δ_x, ratio was set to about 9 giving a maximum mesh size of 0.05 m: in this case, a further grid refinement up to 0.025 m caused much longer computational times but only small variations in the measured rate of spread (<10%).

4. Effect of slope changing on fire propagation

The study of the effect of the terrain slope on the fire propagation rate was already accomplished by the present authors [12]. Results of simulations showed that flames propagate on an inclined surface with a practically constant rate of spread (ROS) and that the ROS increases as the terrain inclination increases. Slope and wind affected the rate of spread in a similar way: however, the ROS had a power-law dependency on wind velocity, while it was almost linearly dependent on the inclination of the domain.

To extend the previous cases to a more complex situation, a double-slope plane geometry was considered in this study in order to analyze the behaviour of a fire front when it moves on a surface which undergoes a sudden variation in the inclination. To validate the capability of WFDS to simulate the fire propagation in such a condition, simulations have been compared with experimental results obtained by Viegas et al. [17] with a dihedral plane; the configuration, used in the experiments and reproduced in the simulations, of the two planes forming a double-slope surface is shown in Figure 1.

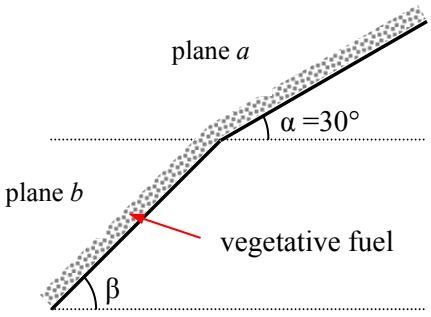

Figure 1. Double-slope plane configuration.

Figure 2: Dihedral plane during a fire test [17]

The actual dihedral table (4m x 4m each plane) used in the experiments is shown in Figure 2. It can form a ridge, a plane slope of constant inclination or a valley that, as the ridge, can be either symmetric or asymmetric. In the fire tests performed by Viegas et al. [17], a load of 0.6 kg/m^2 of straw, having an average moisture content of 6%, was used as vegetative fuel. These data were used in the model while the physical properties of the fuel were deduced from elsewhere [25]. In particular, it was assumed a bulk density of 6 kg/m^3 implying a 10 cm thick fuel bed. In the experimental tests, to ignite the straw a line fire was lighted at the edge of the plane *b* (Figure 1) using a wool thread soaked in a mixture of diesel and petrol fuels, in a 3 to 1 proportion, to assure a practically instantaneous linear ignition. In the simulations a linear 15 cm wide ignition source at the edge of the plane *b* (Figure 1) was considered: maximum heat flux release rate associated to the ignition source was set to 1000 kW/m^2. In order to study the variation of ROS on the plane *a* due the changing of the angle β, in the experimental tests α had a fixed value (30°), while β was varied in the range from -40° to +40°. Negative angles for the plane *b* correspond to a valley configuration.

The comparisons between the experimental and modelled results are shown in Figures 3 and 4. In particular, Figure 3 reports the rate of spread (ROS_B) on the plane *b* evaluated as linear distance run in the time by the fire front along the longitudinal axis of the plane; Figure 4 shows the variation in the rate of spread on the plane *a* (ROS_A), which has a constant inclination (30°), as a function of the slopes adopted in the preceding plane *b*. Figure 3 shows a good agreement between the experimental and predicted values when a fuel load of 0.6 kg/m^2 was assumed. With a heavier vegetative load (1.2 kg/m^2) the ROS had the same behaviour for negative values of the *b* slope, while lower rates of spread with respect to the previous case were found at zero and positive *b* plane inclinations. Figure 3 also shows that the ROS increases at increasing slope. However, when the flames move downwards (β<0°) both the predicted and the observed rate of spread yielded small variations (Figure 3): in these cases the flames are tilted backward and are unable to pre-heat the unburnt fuel. As a result, the experimental rate of spread at -40°<β<-10° exhibits an average constant value of about 0.01 m/s and predictions match this value.

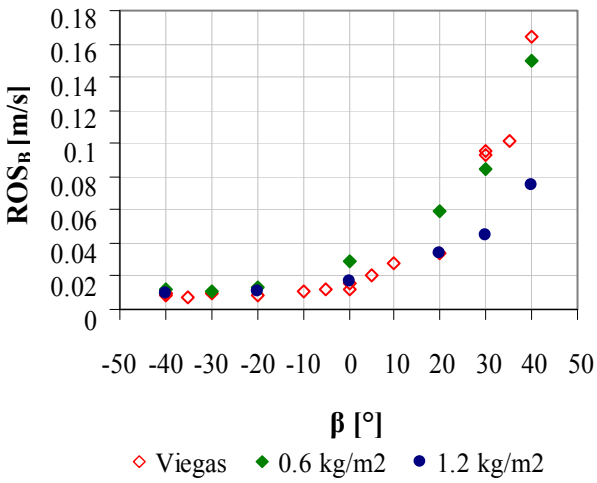

Figure 3. Comparison between the experimental and simulated rate of spread for flames moving on plane *b*

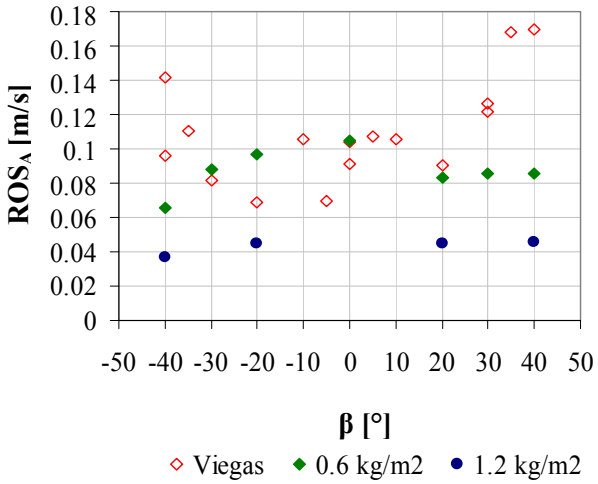

Figure 4. Comparison between the experimental and simulated rate of spread for flames moving on plane *a*

The comparison between simulated and experimental results (Figure 4), assuming a 0.6

kg/m^2 fuel load, shows some differences for β<–30° and β>20°. Actually, experimental results are quite scattered in the whole range of considered inclination angles but they seem to suggest that the ROS_A increases either as β increases or as β decreases with respect to the value measured at β ≈ 0. Instead, the values of ROS_A derived from the simulations increase in the range of β from –40° to 0° and are almost constant in the range 20°<β<40°.

In order to elucidate these findings in Figure 5 the predicted fire front shapes, represented by the 300°C isotherms, are shown: the flame profiles are symmetrically represented with respect to the longitudinal axis (y) and are depicted according to a top view considering an orthographic projection on flat surface (x-y). They show an increasing distortion over time as the fire travels along the combustion table, more pronounced at higher β values. It is also evident how the sudden change of slope, when it occurs, produces a variation of the shape of the fire perimeter.

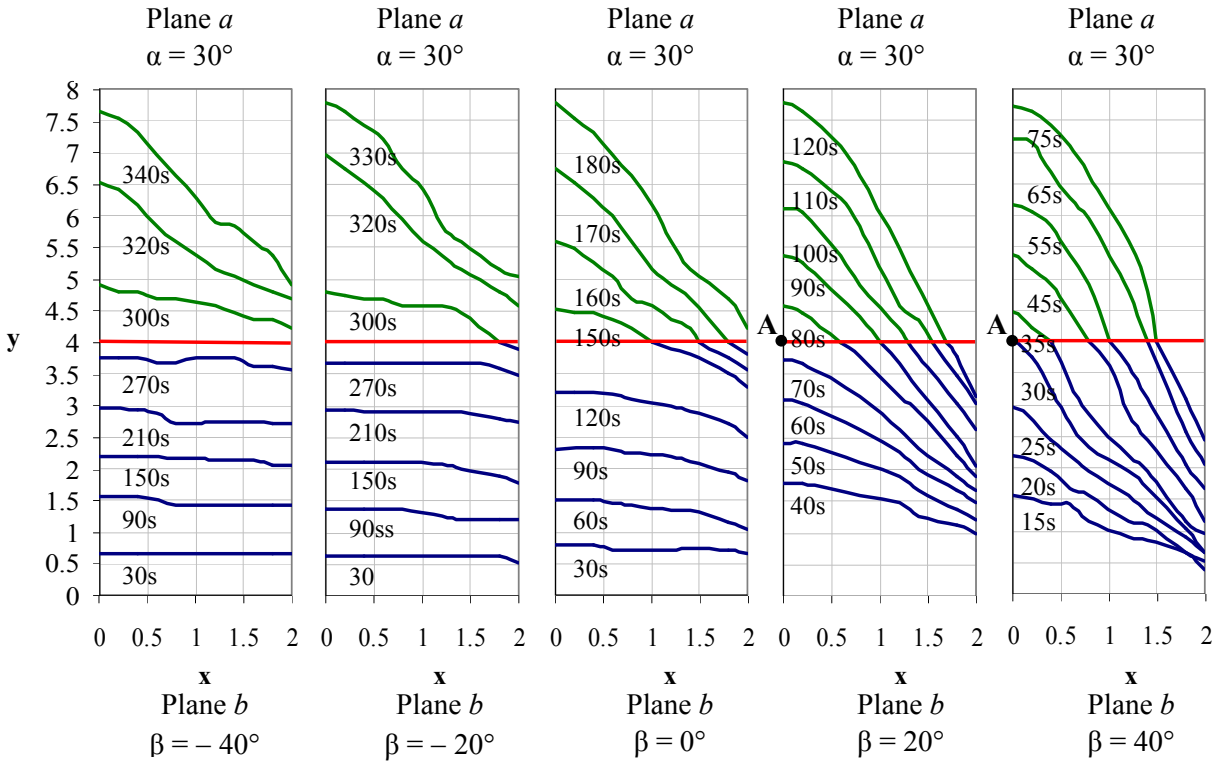

Figure 5. Evolution in time of the fire profiles. Red line marks the changing in slope between the two faces forming the dihedral table. Time in seconds is reported for each profile.

The slope of the plane *b* strongly affects the way the plane *a* becomes ignited: for –20°<β <–40° the transverse flame profile is almost flat before entering the plane *a* while at 20°<β<40° a sort of point ignition source, originating in the centre of the edge of the plane *a*, (point A in Figure 5) is produced. Due to the different β, the heat sources which ignited the plane *a* are characterized by different shapes and intensities and, therefore, originate different ROS_A, as observed in Figure 4.

In Figure 6 the heat released by the fire before moving on the plane *a* is shown for β=–20° and –40°: it can be seen how the energy generated when β is –20° is higher than when it is –40°, explaining the lower ROS_A calculated in this latter case. Instead, when β is equal to 20° or 40° (Figure 7) the ignition source originating on the centre of the edge of the plane *a* (position A in Figure 5) generates nearly the same energy variation (about 14 kW/s) for about

10 seconds after the flame has reached the plane *a*. Therefore, in both cases a very similar heat source ignited the plane *a*, justifying the same ROS_A (Figure 4). When β=0° the result is in between the two previous being the heat source induced on the plane *a* represented by a line that ignites only the central part of plane.

It can be concluded that small variations in the shape of the flame before the plane transition can have important consequences on ROS_A, hence, the discrepancies between the experimental and simulated fire contours seem to justify the different value of rate of spread on plane *a* found by simulations and experiments especially at very steep slopes.

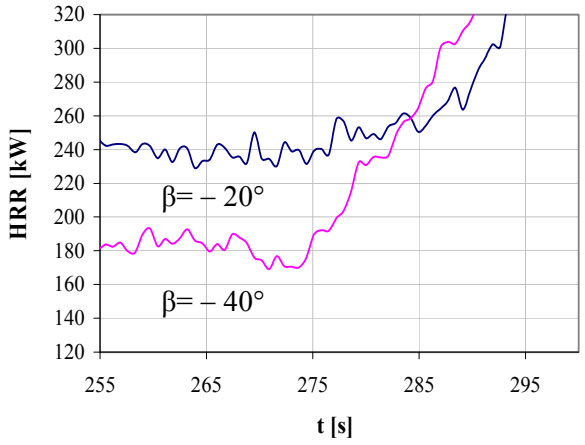

Figure 6. Heat Release Rate (HRR) vs. time on the plane *a* for β=–20° and –40°.

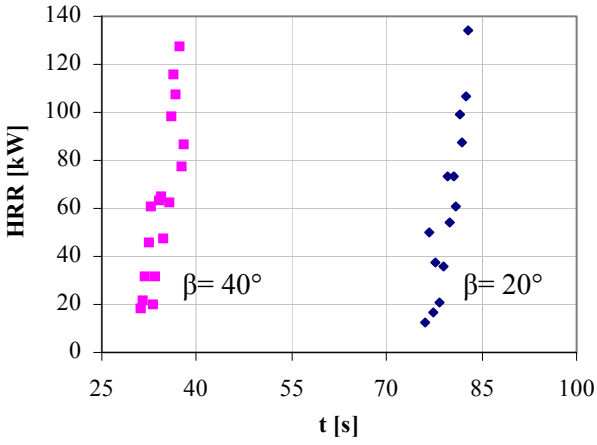

Figure 7. Heat Release Rate (HRR) vs. time on the plane *a*, at β= 20° and 40°. Plane *a* ignition time: 30s and 75s at β= 40° and 20°, respectively

5. Canyon simulation results

For the modelling of a fire developing in a canyon, a geometry built with two adjacent planes (1.5 m x 3 m each) was considered. As shown in Figure 8, each plane was oriented in such a way to form with the horizontal plane two angles (β and δ) each equal to 40°. The physical characteristics of the vegetative fuel (*Pinus Pinaster* needles) covering this surface were taken from the works of Viegas and Pita [18] and Mell at al. [26].

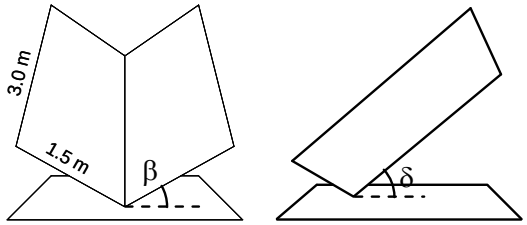

Figure 8. Canyon Configuration (β=δ=40°)

Pine needles were ignited in correspondence of the symmetry plane of the canyon by a pseudo-punctual source ($3.6*10^{-3}$ m^2) at about 1 m from the lower external edge. Fuels having different moisture content (MC) of 0.04, 0.08 and 0.13 on dry basis were considered in the

simulations; the maximum heat release rate associated to the ignition source was set equal to 500 kW/m^2 when the moisture contents were 0.04 and 0.08, and equal to 2000 kW/m^2 when MC was 0.13. All the simulations were run in the absence of wind. In Figure 9 a qualitative comparison between the simulation and experimental [18] results, obtained with a vegetative fuel having MC=0.13, is shown. Figure 9 shows that there are differences between the evolution in the time of the shape of the fire fronts calculated by WFDS and that determined by visual observations and reported in the literature [18]. Specifically, WFDS yields a fire perimeter with an "U" profile, while a "V" shape can be observed from the pictures. However, such a difference could be due to the limitation to display data generated by the computational code. Indeed, the fire shape was obtained from the simulation results considering only the heat released by the burning fuel, i.e. neglecting the visible light radiation present in the actual combustion phenomenon.

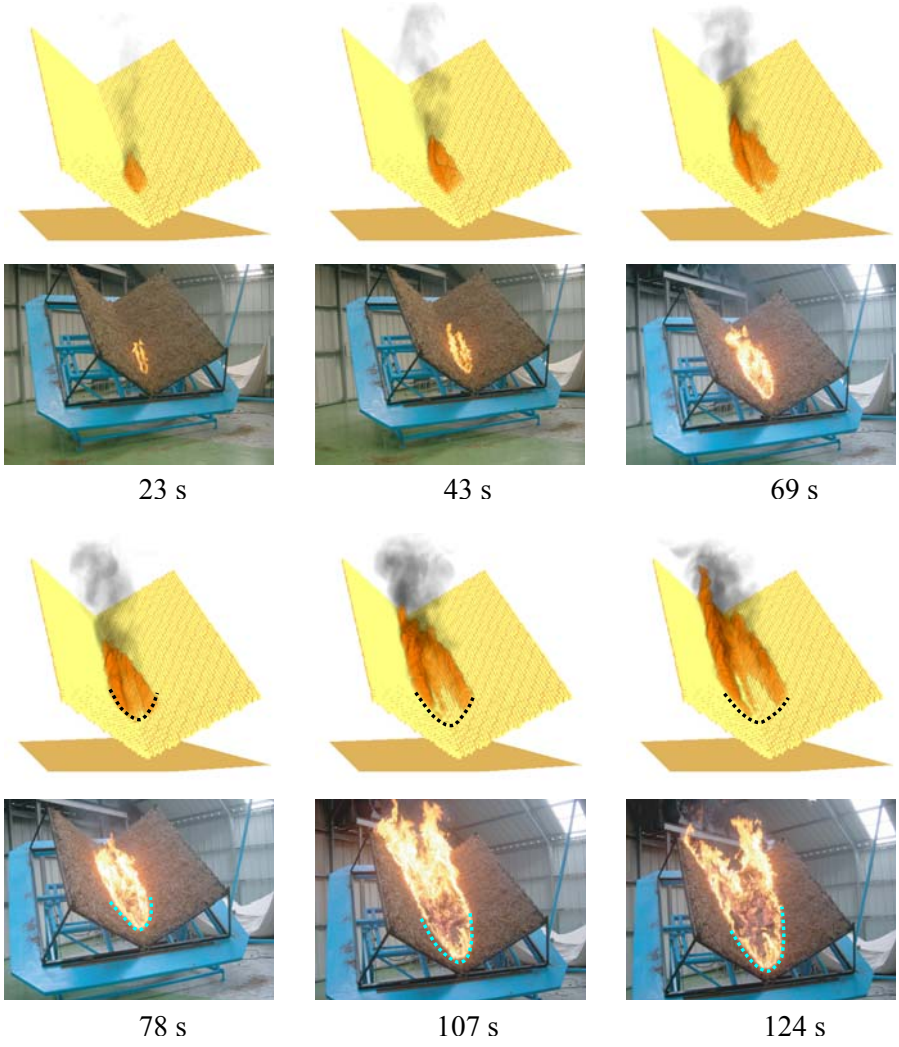

Figure 9. Comparison between experimental and simulation results (MC=0.13). Dotted lines, in snapshots at 78, 107 and 124 seconds, evidence the different fire contours between the experimental and simulation results.

A more quantitative comparison between the experimental and the simulation results is presented in Figure 10 in terms of burned area growth versus time. In this case the burnt

areas, calculated from the isosurfaces of the heat release rate (20 kW/m^3) at ground level, approximate quite well the experimental profile when MC= 0.13 and MC=0.08 (Figure 10). Furthermore, it has to underline that in the work of Viegas and Pita [18] the number of available parameters for defining the vegetative fuel characteristics was limited and, therefore, further information about the fuel characteristics required by the software were taken from a different reference [26].

Besides the results above, Figure 10 shows other two features of the system investigated. The first is the effect of fuel moisture content on the calculated ROS. Indeed, the Figure indicates that the fuel humidity level heavily influences the ROS. Therefore, the lack of accurate information on the values of parameters employed in the experiment could give rise to large differences between modelling and experimental results. The second is that the fire propagation rate has a not linear trend versus time. This can be also appreciated from Table 2 where the parameters of the exponential curve fitting the burnt area values and shown in Figure 10 are reported.

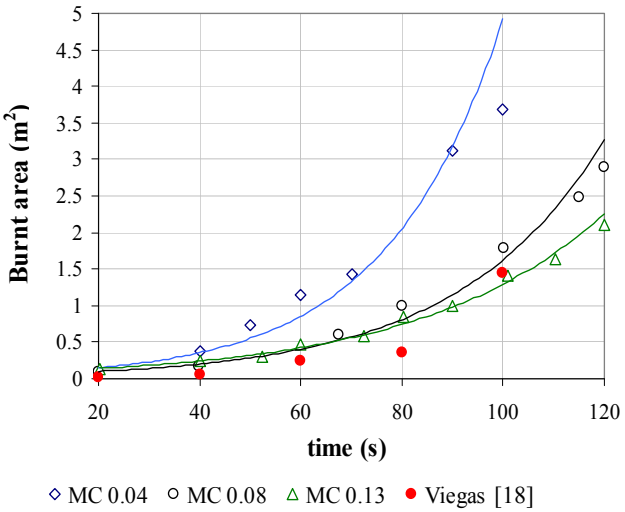

Figure 10. Comparison of burnt area growth in canyon configuration between the experimental tests and the simulated results at different moisture contents. Exponential fitting curves are represented by solid lines.

Table 2: Parameters for the fitting curves in figure 7

Fitting equation: $Area = a \cdot e^{b \cdot t}$ (Area [=] m^2 t [=] s)			
	a	b	R^2
MC= 0.04	0.062	0.0438	0.9572
MC= 0.08	0.0497	0.0349	0.9868
MC= 0.13	0.0802	0.0278	0.991

This finding agrees with the result of Viegas and Pita [18] who experimentally proved that in this domain configuration the fire has a peculiar dynamic behaviour: the rate of spread increases continuously, even in the absence of wind, causing the well known phenomenon of blow-up associated with real canyon fires.

The unreaching of steady state conditions for ROS in the case of canyons could be explained considering that this particular geometrical configuration gives rise to an exposition of the vegetal fuel to radiative and convective heat anticipated with respect to the arrival of the front flame. Such an exposition warms and dries the vegetal fuel and, when the flame front reach it, the fuel is ready to burn generating much more energy with respect to the case where part of the generated power is spent to warm and evaporate water. This lead to an increase of the rate of combustion and, then, of the rate of spread. This interpretation agrees with suggestions from the literature [27] and is also supported by the results of net power generated by the burning system in the time reported in Figure 11. In this Figure the net power coming out from the calculation domain, in the cases of three different MC of the fuel, is reported as a function of the time. As expected, the absolute value of the net HRR decreases at increasing fuel moisture content because, for a given load, an higher MC reduces the amount of fuel available for burning and, correspondingly, increases the quantity of water to be evaporated. The particular form of the curve pertaining to MC 0.04 is due to the rapid consumption of the flammable material. From the Figure it is evident, however, that whatever the MC, the trend of the net power generated increases more than linearly in the time reflecting the trend already observed for the burned area (Figure 10). The peculiarity of results in Figure 11 can be appreciated when they are compared with the same quantities obtained in the case of flat terrains. In this latter case, as reported in a previous work [12], apart from a short initial transient the net power coming out from the domain is practically constant.

Obviously, the total balance between the energy that can be generated by the fuel and the energy necessary to warm up and dry the fuel and the terrain must be the same whatever the terrain slope. This implies that initially the net power generated by the burning of a canyon area is much lower than that pertaining to a flat terrain. On the basis of the above considerations it must be concluded that also the time becomes an important factor in describing the fire behaviour and its role must be considered along with the topography, vegetation and meteorological parameters.

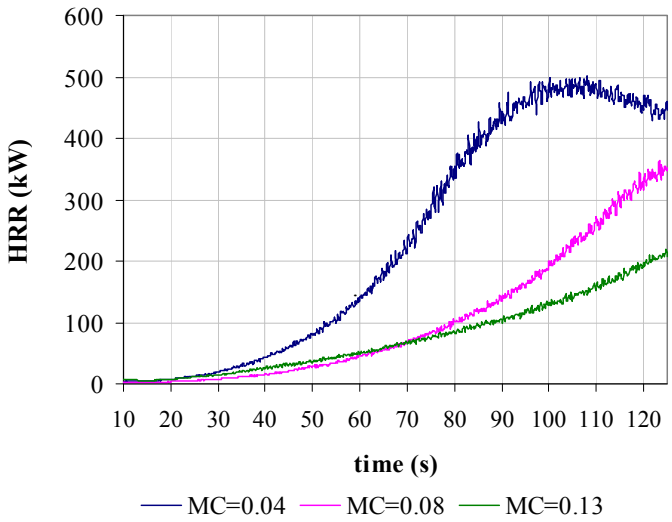

Figure 11. Heat release rate profiles for canyon geometry at different moisture content (MC)

6. Conclusions

The ensemble of the results clearly showed that the physics-based model and code WFDS, specifically designed to simulate the wildfire behaviour, is an effective tool to study the way the flames spread across different kinds of terrains.

The results obtained for the double-inclination domain showed that the fire spreading rate is dependent not only of the fuel bed properties and the terrain slope but also of the boundary conditions, namely, the fire spread properties at the edge of the given fuel bed. Specifically, changes in the inclination of a terrain *b* preceding a further terrain *a*, whose inclination is constant, produce ignition sources on the terrain *a* having different shapes and energies, giving rise, then, to different ROS_A. The agreement between experimental and simulated results was satisfactory but failed partially when considering high βs (both positive and negative).

The dynamic behaviour of the fire was also analyzed. In particular, in the canyon configuration it was observed that the fire growth is relatively slow at the beginning, and then increases very rapidly and the time lag for this transition depends on the moisture content and on the fuel properties.

7. References

[1] Albini F.A.: "A model for fire spread in wildland fuels by radiation", *Combustion and Science Technology* 42: 229–258 (1985).

[2] Albini F.A.: "Wildland fire spread by radiation: a model including fuel cooling by convection", *Combustion and Science Technology* 45: 101–113 (1986).

[3] Burgan R.E., Rothermel R.C.: "BEHAVE: Fire behaviour prediction and fuel modeling system: fuel subsystem. General Technical Report", *INT-167, USDA Forest Service, Intermountain Forest and Range Experiment Station, Ogden, Utah*, (1984).

[4] Gwynfor D.R.: "Numerical simulation of forest fires", *International Journal for Numerical Methods in Engineering* 25: 625–633 (1988).

[5] Weber R.O.: "Towards a comprehensive wildfire spread model", *International Journal of Wildland Fire* 1(4): 245–248 (1991).

[6] Hanson H.P., Bradley M.M., Bossert J.E., Linn R.R., Younker L.W.: "The potential and promise of physics-based wildfire simulation", *Environment Science Policy*, 3: 161-172 (2000).

[7] Linn R.R., Reisner J., Colman J.J., Winterkamp J.: "Studying wildfire behavior using FIRETEC", *Int. J. Wildland Fire*, 11: 233–246, (2002).

[8] Mell W., Charney J.J., Jenkins M.A., Cheney N.P., Gould J.: "Numerical simulations of grassland fire behavior from the LANL-FIRETEC and NIST-WFDS models". *Proc. EastFIRE Conference*, May 11-13, Fairfax (VA), 10 pp., (2005).

[9] Mell, W.E., Jenkins. M.A., Gould, J.S., Cheney N.P.: "A physics-based approach to modeling grassland fires", *International Journal of Wildland Fire*, 16: 1-22 (2007)

[10] Mell W., Maranghides A., McDermott R., Manzello S.L.: "Numerical simulation and experiments of burning douglas fir trees", *Combustion and Flame*, 156: 2023–2041 (2009).

[11] Morvan D., Dupuy J.L.: "Modeling the propagation of a wildfire through a Mediterranean shrub using a multiphase formulation", *Combustion and Flame* 138: 199–210 (2004).

[12] Malangone L., Russo P., Vaccaro S., "Effects of wind and terrain slope on flames propagation in a vegetative fuel bed", Submitted to the XXXIV Event of the Italian Section of the Combustion Institute (2011).

[13] Viegas, Domingos X.: "On the existence of a steady state regime for slope and wind

driven fires", *Int. J. of Wildland Fires*, 13, 101-117 (2004).
[14] Rothermel C.: "A mathematical model for predicting fire spread in wildland fuels", in: Research Paper INT-115: US Department of Agriculture, Forest Service, Intermountain Forest and Range Experiment Station, Ogden, UT, 1972, p. 40.
[15] Boboulos, M., Purvis, M.R.I.*:* "Wind and slope effects on ROS during the fire propagation in East-Mediterranean pine forest litter", *Fire Safety Journal,* 44: 764–769 (2009).
[16] Viegas, Domingos X.: "Slope and wind effect on fire propagation". *Int. J. of Wildland Fires*, 13: 143-156 (2004).
[17] Viegas D. X., Rui Figueiredo A., Pita L.P., David D., Rossa C.: "Analysis Of The Changes Of Boundary Conditions In A Slope". *Proc. VI International Conference on Forest Fire Research*, D. X. Viegas (Ed.) (2010).
[18] Viegas D. X., Pita, L.P.: "Fire spread in canyons", *Int. J. of Wildland Fires*, 13, 253-274 (2004).
[19] Hinze J.O.: *Turbulence*. 2nd Edition. McGraw-Hill, 1975.
[20] McGrattan K., Hostikka S., Floyd J., Baum H., Rehm R., Mell W., McDermott R.: "Fire Dynamics Simulator (Version 5) Technical Reference Guide - Volume 1: Mathematical Model". NIST Special Publication 1018-5, (Available at: http://www.fire.nist.gov/fds/) , (2010)
[21] Cox, G.: Basic Considerations. In: *Combustion Fundamentals of Fire*. Ed. G. Cox. Academic Press, London, 1995.
[22] Rehm R.G. and Baum H.R.: "The Equations of Motion for Thermally Driven, Buoyant Flows", *Journal of Research of the NBS*, 83: 297–308, (1978).
[23] Zukoski E.E.: "Properties of Fire Plumes", Chapter 3, *Combustion fundamentals of Fire*, G. Cox Editor, Academic Press, Pp.101-220, 1995.
[24] Mcgrattan K., Mcdermott R., Hostikka S., Floyd J.: "Fire Dynamics Simulator (Version 5) User's Guide". NIST Special Publication 1019-5,. Available At: Http://www.Fire.Nist.Gov/Fds/ (2010).
[25] Zhou H., Jensen A.D., Glarborg P., Jensen P.A., Kavaliauskas A.: "Numerical modeling of straw combustion in a fixed bed", *Fuel* 84: 389–403 (2005).
[26] Mell, W.E., Manzello, S.L. and Maranghides, A.: "Numerical modeling of fire spread through trees and shrubs". *Proc. V International Conference on Forest Fire Research*, Viegas Ed., 2006.
[27] Velez R.: "La defensa contra incendios forestales – Fundamentos y experiencias", McGraw Hill Interamericana de España: Madrid, Spain (in Spanish), 2000.